

A NEW WATERMARKING ALGORITHM BASED ON HUMAN VISUAL SYSTEM FOR CONTENT INTEGRITY VERIFICATION OF REGION OF INTEREST

Emad FATEMIZADEH, Mona MANESHI

Sharif University of Technology

Department of Electrical Engineering

Azadi Ave., Tehran, Iran

e-mail: fatemizadeh@sharif.edu, maneshimona@gmail.com

Communicated by Pavel Mautner

Abstract. This paper proposes a semi-fragile, robust-to-JPEG2000 compression watermarking method which is based on the Human Visual System (HVS). This method is designed to verify the content integrity of Region of Interest (ROI) in tele-radiology images. The design of watermarking systems based on HVS leads to the possibility of embedding watermarks in places that are not obvious to the human eye. In this way, notwithstanding increased capacity and robustness, it becomes possible to hide more watermarks. Based on perceptual model of HVS, we propose a new watermarking scheme that embeds the watermarks using a replacement method. Thus, the proposed method not only detects the watermarks but also extracts them. The novelty of our ROI-based method is in the way that we interpret the obtained coefficients of the HVS perceptual model: instead of interpreting these coefficients as weights, we assume them to be embedding locations. In our method, the information to be embedded is extracted from inter-subband statistical relations of ROI. Then, the semi-fragile watermarks are embedded in the obtained places in level 3 of the DWT decomposition of the Region of Background (ROB). The compatibility of the embedded signatures and extracted watermarks is used to verify the content of ROI. Our simulations confirm improved fidelity and robustness.

Keywords: Semi-fragile watermarking, ROI, JPEG2000 compression, content integrity verification, HVS-based perceptual models

Mathematics Subject Classification 2010: 68U10, 94A08, 94A62, 68P25

1 INTRODUCTION

Recently, the introduction of wireless communication technology provided a suitable framework for many other technologies such as telemedicine [1]. The focus of this paper is on data transmission of tele-medical images, which have diagnostic and treatment significance [2].

In image-based diagnosis two major problems exist. First, there are lots of details and fine local information in the transmitted images, which enriches them for diagnostics [3]. The critical need for discriminating image regions led to the introduction of Region of Interest (ROI) and Region of Background (ROB). ROI refers to those regions that carry the most important medical and clinical information, in contrast to other regions of the image, which are called ROB. Second, the critical deficiency of bandwidth and saving capacity in telecommunication techniques also provides problems. Today, many medical images are captured and archived in digital format, and the gray-level radiology images are not exceptional [4]. Without compression, long-term storage and transmission of these images through mobile tools is not possible. Effective lossy compression of these images allows for increased transmission speed and decreased archiving costs.

The content integrity control of such images, especially their ROI, after the decrease in their quality due to tele-communication system defects, especially lossy compression distortions, makes us to consider some means to overcome these problems. Watermarking can be used as an effective tool to satisfy this goal [5]. Watermarking is a method of invisibly altering data to embed a message [6].

Here, content integrity confirms or denies the authentication of an image or part of it against all kinds of manipulations [7]. Manipulation can vary between admissible and impermissible activities such as different kinds of image processing methods to all kinds of the intentional attacks. In content integrity verification, the watermarking algorithm resists predefined allowable or not allowable manipulations and breaks against more than those values. These kinds of watermarking techniques usually are semi-fragile, and the applied method evaluates the amount, type, and location of manipulation [8]. Sometimes, semi-fragile watermarking is defined as a subset of fragile watermarking, which resists against some changes such as compression or quantization noise and breaks in other ways.

Watermarks should be as imperceptible as possible while robust to compression. Progress of this issue relates to the development of compression methods based on human visual system (HVS) [9]. This direct relationship results from the fact that compression is not basically apart from the elimination of redundancies and quantization. The human eye, because of its structure and information processing, is itself an efficient and well-built compressor [10]. Thus, if we can discern the eye's ability and inability points in the elimination or amplification of details, we could develop more effective compression methods.

The work proposes a semi-fragile, robust JPEG2000 compression and HVS-based watermarking method that is designed to control the content integrity of ROI in teleradiology images. This method is based on Xie's perceptual model [11] and

the replacement of watermarks in the discrete wavelet transform (DWT) domain. On the transmitter side, the information to be embedded is extracted from the inter-subband statistical relations of the ROI and are then embedded in the ROB. On the receiver side, after extracting the embedded watermark from the ROB and comparing them with the signature bits extracted from the ROI, the accordance of these two is measured with a special predefined threshold. Finally, the content integrity of the ROI is confirmed or denied.

This paper is organized as follows. The next section presents a literature review of research on ROI-based image watermarking. Then, we review Xie's perceptual model in Section 3 and propose our method in Section 4. Finally, the results are shown, and a conclusion is presented in Sections 5 and 6.

2 LITERATURE REVIEW

An investigation targeting watermarking of imagery reveals a plethora of publications incorporating many different modality types [12–15]. These methods were not designed for robust lossy JPEG2000 compression, which is essential for decreasing the size of medical images. The general goal of those techniques is to ensure that the watermark endures manipulation without damaging the value of the work [16, 17]. However, these approaches do not address the need of authenticating critically important image regions. Complementary methods which verify the integrity of crucial diagnostic information against compression methods include ROI-based watermarking techniques [18, 19].

A well-known publication by Lin and Chang [18] was proposed and practically implemented by Cox et al. [19]. The basis of Lin theory is that not only the sign of differences but also the ratio of two discrete cosine transform (DCT) coefficients, which are located in similar places of two blocks, are unchanged after quantization when JPEG compression is applied. This method can be used to authenticate images by allowing lossy JPEG compression up to an acceptable level and can be designed to survive distortion such as integer rounding, decimation, application specific transform, and image cropping.

Multiple embedding around the ROI is useful when the image is clipped and one watermark is lost. A recent work presented by Osborne [20] uses acceptable levels of lossy JPEG compression to discuss DCT coefficients while maintaining diagnostic integrity. The results of testing the quality performance of the multiple ROI watermarking system show that the technique outperforms earlier methods such as that of Lin and Chang with improved image fidelity. Moreover, JPEG quantization experiments also show that the watermark will remain embedded in the image after increased levels of JPEG quantization.

Most current research is related to watermarking in the DWT domain. The most important reason for using DWT is its compatibility with HVS [21]. The hierarchical and pyramidal structure of this transformation gives very exact local information. Unlike DCT, which forces to segment the image into blocks in order to obtain lo-

cal information, DWT gives local information in different frequency intervals of the image. In this way, one can select the edges and active areas from those of smooth regions and add the watermarks only to the edges of these busy areas. Another reason for its use is the wide application of wavelets in new compression strategies [22]. The use of this transformation in new standards such as JPEG2000 and MPEG4 would provide good compatibility with available watermarking and compression systems; this harmony improves the ability to correctly detect watermark signals after their passage through communication channels.

Other techniques that have been proposed to authenticate ROI regions in the DWT domain include works by Wakatani [23], who proposed to embed multiple signature information around a known ROI. In this article, the most significant information was embedded into the region closest to the ROI in a spiral way. This system was intended for application over web-based medical image database systems rather than wireless end applications.

Another scheme was proposed by Lie to robustly watermark lossy JPEG2000 ROI compressed images [24]. A dual watermarking scheme was proposed in the DWT domain with one watermark being naturally fragile and the other robust. These schemes were designed to be embedded separately into the ROI and ROB.

Future work involving ROI watermarking has been proposed in a paper by Lee [25], based on exploiting the properties of wavelet coefficient signs experimentally found to be invariant to lossy compression standards including JPEG and JPEG2000.

In this research, we first review the algorithm proposed by Xie [11]. Briefly, his method is designed to embed robust watermarks in the DWT domain with the aid of additional processes. His watermarking system is not ROI-based and thus is not suitable for content integrity verification. However, his perceptual model is simpler and more applicable than earlier models. In the next section, we will briefly review his method.

3 XIE PERCEPTUAL MODEL

Lewis's method [26] for quantizing DWT coefficients by matching local noise served as a foundation for Xie's robust watermarking system. Lewis's method was based on the estimation of noise sensitivity in HVS. One of its direct applications is in image compression techniques.

Lewis believed that traditional compression methods, which are based on eliminating redundancies, led to low compression rates. He looked for novel techniques that were more than a simple eliminator. These methods should not create any serious problems in image quality, especially in areas which are more important from a perceptual point of view, like edges. Lewis claimed that the errors caused by these manipulations during the compression process could be modeled as noise. He also found effective factors in eye sensitivity to this noise by implementing psychophysiology. He introduced the following three factors [26]:

- background illumination
- frequency band
- texture activity.

Xie approximates Lewis’s perceptual model as follows. According to Xie’s method [11], we decompose the host image, $I(x, y)$, up to three levels in the DWT domain (Figure 1).

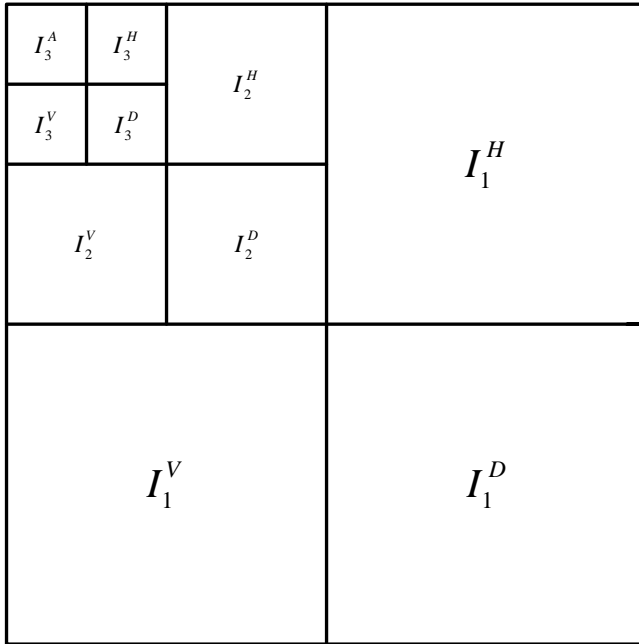


Fig. 1. 3 level 2-D wavelet decomposition of image

For simplification, we assume that each subband in each level is represented by $I_l^\theta(i, j)$, where $l \in \{1, 2, 3\}$ is the level of decomposition and $\theta \in \{LL, LH, HL, HH\}$ is the sub-band orientation written as $\theta \in \{a, h, v, d\}$. The weighting function, $W_l^\theta(i, j)$, is defined as:

$$W_l^\theta(i, j) = \Theta(l, \theta)\Lambda(l, i, j)[E(l, i, j)]^{0.2}. \tag{1}$$

We should emphasize that the relation of the weighting value and eye sensitivity is reversed; i.e. the more the weighting function, the less the eye sensitivity.

The first term in Equation (1) indicates how eye sensitivity varies according to the level and orientation of decomposition and is calculated as follows:

$$\Theta(l, \theta) = \Theta_l(l)\Theta_\theta(\theta) \tag{2}$$

where $\Theta_l(l)$ and $\Theta_\theta(\theta)$ are defined as:

$$\Theta_\theta(\theta) = \begin{cases} \sqrt{2} & \text{if } \theta = d \\ 1 & \text{otherwise} \end{cases}, \quad \Theta_l(l) = \begin{cases} 1.00 & \text{if } l = 1 \\ 0.32 & \text{if } l = 2 \\ 0.16 & \text{if } l = 3. \end{cases} \quad (3)$$

The second term in Equation (1) implements the second assumption and estimates the local luminance of each level and subband according to the values of gray level approximate sub-band of that level, $I_l^a(i, j)$.

$$\begin{aligned} \Lambda(l, i, j) &= 1 + L'(l, i, j) \\ L'(l, i, j) &= \begin{cases} 1 - I_l^a(i, j) & I_l^a(i, j) < 0.5 \\ I_l^a(i, j) & \text{otherwise} \end{cases} \end{aligned} \quad (4)$$

Finally, the last term in Equation (1) shows the texture activity in the neighborhood of a pixel and is defined as

$$E(l, i, j) = \frac{([I_l^h(i, j)]^2 + [I_l^v(i, j)]^2 + [I_l^d(i, j)]^2)}{3} \text{var} \{I_l^a(i, j)\}. \quad (5)$$

Each level consists of two terms. The first term is the mean square of the subbands at that level, and the second is an estimation of local variance of the approximate subband in a 3×3 neighborhood of the mentioned pixel at that level. According to this weighting function, Xie associates a certain weight to each watermark and embeds it into the host image. However, in this study, we do not consider these coefficients as weights and use them to find the embedding places instead.

4 PROPOSED METHODOLOGY

Most research on semi-fragile watermarking is fragile in the feature extraction stage [18, 19, 23]. By considering this problem and paying less attention to features, we propose a new method in which the ROI feature extraction is semi-fragile and robust to JPEG2000 compression. Many features were tested, and a six-member set was selected. The final selected feature was the one that led to the highest correct signature extraction percentage and the highest fidelity criteria. We also use the replacement method for embedding, so that extraction can be blind.

First, we decompose the host image with three-level DWT; then, the coefficients of the subbands of level three are extracted. By considering the eye's sensitivity to phase distortion, especially in edges, the linear phase is considered for synthesis and analysis filters in image processing applications. As a result, we applied Daubechies order of 1 (Haar) filter in our experiments.

Watermark, W , indicates inter-subband statistical relations in the ROI. The change of this inter-subband statistical relation depends on the kinds and levels of external manipulations. For example, alteration of this statistical property would

be observable when a considerable part of ROI image is replaced [24]. In contrast to malicious attacks, the statistical property still remains the same or slightly altered after unintended manipulation. Here, the statistical relation, or feature, is defined as:

$$\text{Signature Symbol} = |LL_3(i, j) - HL_3(i, j)| + |LL_3(i, j) - LH_3(i, j)| \quad (6)$$

where 2-tuple (i, j) indicates the pixel position in the third level of wavelet decomposition. For an M by N image, i and j vary from 1 to $\frac{M}{2^3}$ and $\frac{N}{2^3}$, respectively.

Then, extracted signature symbols for each pixel of sub-images are categorized into four sets according to their values. Each category is labeled by using the following rule:

$$L_{LH3}(i, j) = \begin{cases} 0 \text{ symbol } \langle T_0 \\ 1T_0 \langle \text{symbol } \langle T_1 \\ 2T_1 \langle \text{symbol } \langle T_2 \\ 3T_2 \langle \text{symbol} \end{cases} \quad (7)$$

where $T_0, T_1,$ and T_2 stand for three partition thresholds and $L_{LH3}(i, j)$ denotes the label for each pixel with position (i, j) in the ROI. Similarly to the signature symbol, 2-tuple (i, j) indicates the pixel position in the third level of wavelet decomposition. For an M by N image, i and j vary from 1 to $\frac{M}{2^3}$ and $\frac{N}{2^3}$, respectively. $L_{LH3}(i, j)$'s are converted into binary bits and concatenated to form the watermark, W . It is important to select proper thresholds T_i so as to make tradeoffs between fragility and robustness of the ROI content change. One may use uniform partition of possible values of the *Signature Symbol*.

Investigations and several tests on different benchmark images show that the method does not work properly in images with different luminance. The generation of bits 0 and 1 should not be dependent on the reference image, since most of the time we have no information about the host image's brightness level. Thus, thresholds should be selected, which leads to equal generation probability of bits 0 and 1. By using the probability density function of the *Signature Symbol*, we select boundaries so that the enclosed area between each pair of adjacent thresholds is 0.25 (Figure 2). In this way, the number of symbols 0 to 3 would be the same; since the number of total 0 and 1 bits in their binary display is the same, the total number of generated 0 and 1 bits is the same. Moreover, there is no need to know T_i on the receiver side, and this method shows better robustness against compression and thus an improved correct watermark extraction percentage.

For embedding the watermarks, we choose level 3. The robustness of this level against compression is better than that of lower levels, and its embedding capacity is good. By embedding the watermarks in places where eye is less sensitive to them, the fidelity becomes better. We used Xie's weighting function to give weight to each coefficient in the DWT domain at level 3 and select the threshold that contains 75% of them. We select the remaining 25% that are larger than this threshold. These coefficients are those to which eye has the least sensitivity, thus, their location in the DWT domain is an ideal place for embedding the watermarks. Both fidelity and robustness improve in this way (Figure 3).

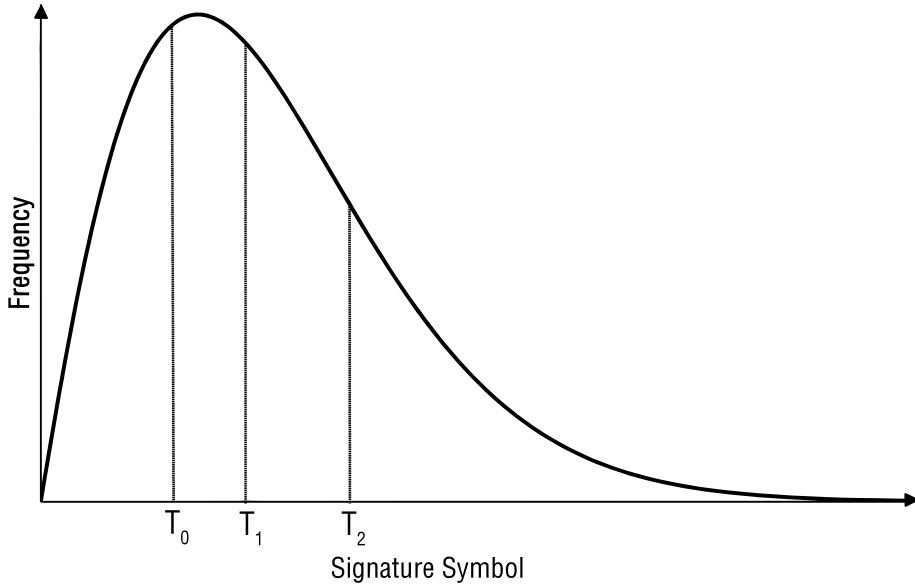


Fig. 2. Probability density function of signature symbol

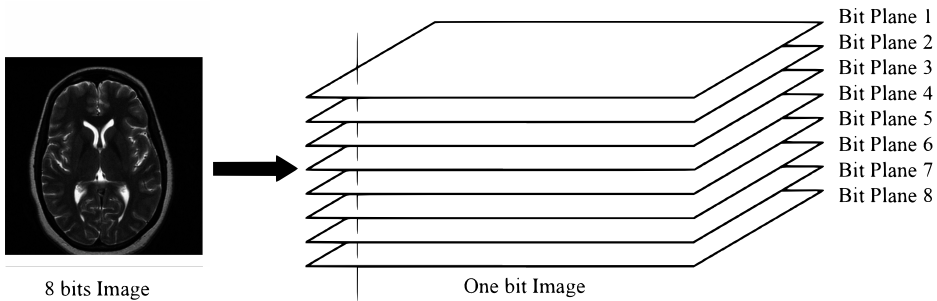


Fig. 3. Bit plane decomposition of a sample image

Using the replacement method, the obtained signature bits, W , are embedded into the coefficients of the bit planes (Figure 3) of LH3 and HL3 sub-bands of the ROB at the pre-assigned locations. We do not embed any watermark in HH3, since it is very sensitive to compression and breaks easily against distortion. To ensure that the ROB in the selected resolution level has adequate embedding capacity, we choose adequate bit planes to embed W completely. Denoting any bit plane chosen for W embedding as α , we calculate its embedding capacity C_α and then embed W into the most top bit plane that has a C_α larger than N (the length of W).

The extraction steps are reversed in order, and the extracted signature from ROI is compared in a bitwise identical manner with the extracted watermark from the

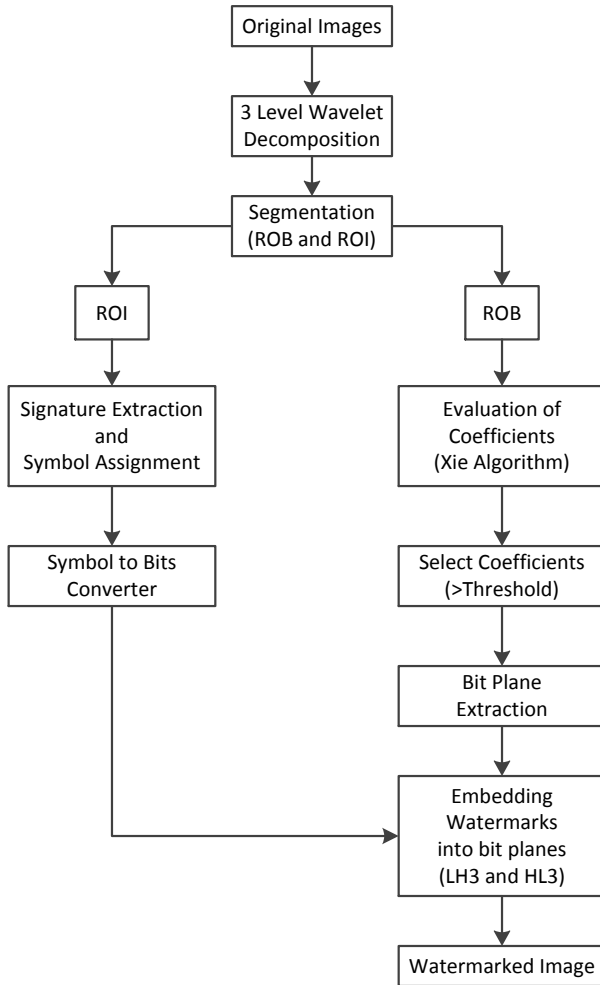


Fig. 4. Block diagram of the proposed method

ROB. The relative number of matched bits to total bits is compared with a threshold, π . If the adaptation percentage according to normalized Hamming distance is more than or equal to π , then ROI content integrity is verified. Ideally, π should be 1.0; however, due to rounding and quantization error during the compression process, we propose 0.85. This threshold was chosen through trial and error study on a large dataset. The block diagram of our proposed method is shown in Figure 4.

5 RESULTS AND DISCUSSION

Evaluation of the proposed method consists of general and specific tests. General tests include compression tests with two different criterions: fidelity and robustness. Specific tests include other types of tests related to parameters and specific characteristics of the method. Since the transformation domain is DWT, the invariant variable in the compression test is the output bit rate or BPP (bits per pixel). Reasonably, the compression test with fidelity criterion measures $PSNR$ or $\Delta PSNR$ in the output image per BPP and the compression tests with robustness criterion measure the correct watermark extraction percentage (CWEP) or correct signature extraction percentage (CSEP) per BPP. CWEP and CSEP are defined as normalized distance between embedded and extracted watermark and signatures, respectively. Peak signal-to-noise ratio ($PSNR$) as an index of compression fidelity criteria is defined as follows:

$$PSNR(I, I_W) = 10 \log_{10} \left[\frac{\max_{\forall(x,y)} I^2(x,y)}{\frac{1}{N_I} \sum_{\forall(x,y)} (I_W(x,y) - I(x,y))^2} \right] \quad (8)$$

where I is the host image, I_w the watermarked and compressed image, (i, j) pixel coordination, and N_I is the number of pixels in I or I_w . $\Delta PSNR$ is defined as

$$\Delta PSNR = PSNR(I, I_C) - PSNR(I, I_W) \quad (9)$$

where I_C is the reference compressed image. This criterion measures the amount of fidelity decrease in the compressed watermarked image due to watermarking. CWEP and CSEP measure the normalized Hamming distance between the embedded and extracted watermarks and between the embedded and extracted signatures, respectively. CWEP and CSEP point to the robustness of the watermarking system and the applied feature in the extracting signature, respectively. CWEP and CSEP are defined as:

$$CWEP = \frac{\sum_{i=1}^M W(i) \oplus W^*(i)}{M} \quad (10)$$

$$CSEP = \frac{\sum_{i=1}^M S(i) \oplus S^*(i)}{M}$$

where W^*/S^* are the extracted watermark/signature), W/S are the embedded watermark/signature, M is the length of the string, and \oplus is *exclusive or* operator.

For our preliminary simulations, we chose a Magnetic Resonance Image (MRI) with 256×256 size. The ROI was defined in the middle of image with a size of 113×113 . A sample image and the resulting watermarked image are shown in Figure 5.

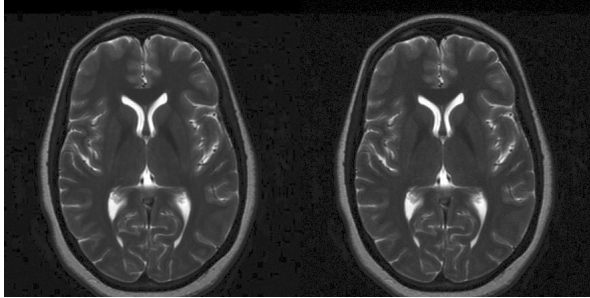


Fig. 5. Original image (Left) and watermarked image (Right) by the proposed method

5.1 Results of General Tests

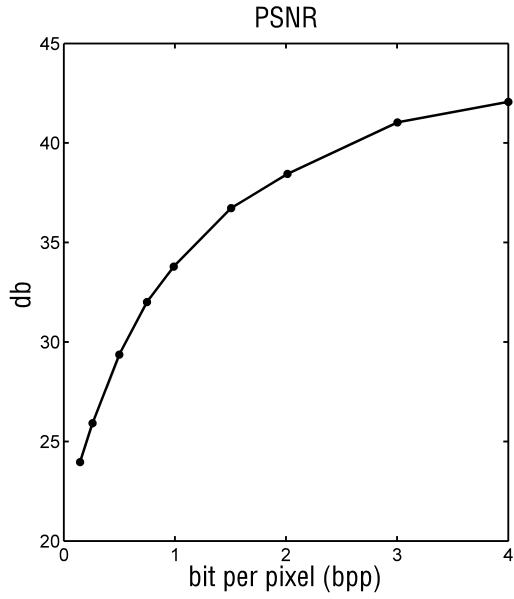
Figures in this part show the result of the compression test with robustness and fidelity criterions. It is obvious from Figure 6 that by increasing BPP, $PSNR$ will also increase. By increasing BPP, we are allocating a longer code for each pixel; thus, less distortion is expected during the compression process. High $PSNR$ values demonstrate the efficiency of our method in making only small changes in the visual quality of the output image and thus image fidelity. The watermarking distortions are less comparable to the compression distortions in low BPPs. This fact is also clear by $\Delta PSNR$ figure. By increasing BPP (less compression), $\Delta PSNR$ will decrease.

An advantage of our proposed method is the high values of CSEP (over 94%) because of its robust to compression ROI features. It is also clear from Figure 7 that the content integrity is verified for BPPs of more than 2 (CWEP is greater than 85%). In the large dataset for BPPs over 1.5, the CWEP is greater than 85%.

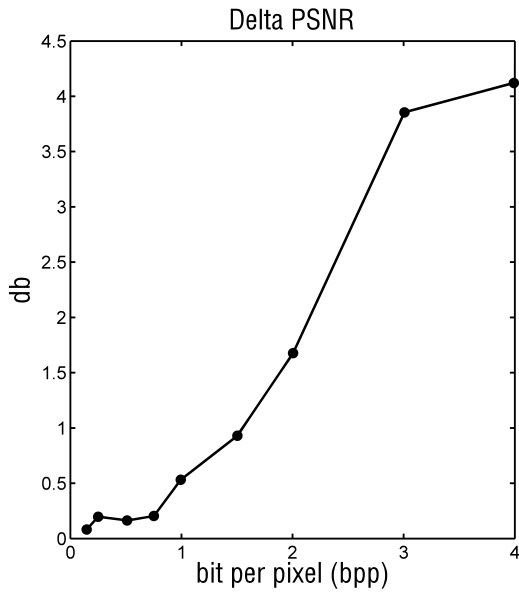
5.2 Results of Specific Tests

We perform several experiments to find the effect of changing the embedding bit plane, the ROI extracted features, and the percentage of eliminated coefficients. The embedding bit plane can range from 0 to 5. We ignored less significant bit planes (6 and 7), since their embedding would be too fragile. We propose six robust ROI features that are appropriate for our application in Table 1.

The elimination percentage points to the percentage of those weighting coefficients were discarded after applying the HVS-based model. We expressed this definition by the means of cut off frequency. For example, the cut off frequency equal to 75% means that only 25% of higher weights (to which the eye is less sensitive) are kept for embedding. Figure 8 shows that by increasing the embedding bit plane the quality of output image improves. By increasing the embedding bit plane from 0 to 5, $PSNR$ improves, since watermarks are embedded in less important bits of image, and thus its distortion is less perceptible, meanwhile $\Delta PSNR$ shows the

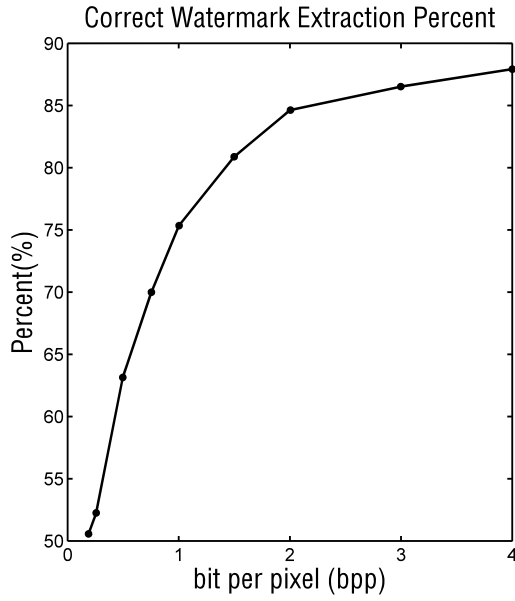


a)

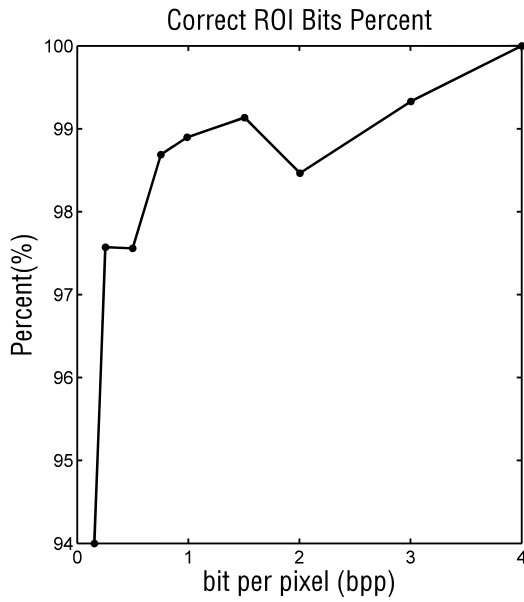


b)

Fig. 6. a) $PSNR$ and b) $\Delta PSNR$ as a function of BPP in bit plane #3



a)



b)

Fig. 7. a) CWEP and b) CSEP as a function of BPP in bit plane #3

Feature	Signature Symbol
1	$ H_3(i, j) - D_3(i, j) $
2	$ 0.5H_3(i, j) + 0.5V_3(i, j) - D_3(i, j) $
3	$ H_3(i, j) - D_3(i, j) + V_3(i, j) - D_3(i, j) $
4	$ L_3(i, j) - D_3(i, j) + H_3(i, j) - D_3(i, j) + V_3(i, j) - D_3(i, j) $
5	$ L_3(i, j) - D_3(i, j) $
6	$ L_3(i, j) - H_3(i, j) + L_3(i, j) - V_3(i, j) $

Table 1. Set of extracted features from ROI

opposite. The reason is that by increasing the embedding bit plane, the destructive effect of watermarking is comparable to those of compression, so their difference ($\Delta PSNR$) decreases.

The display of CWEP in the sample image with different bit planes in BPP1 is shown in Figure 9. As expected by increasing the embedding bit plane, the CWEP decreases with a high slope, since the watermarks are embedded in places that are very sensitive to compression. Since the change in the embedding bit plane has no effect on the ROI and only relates to the ROB, we do not show any test results for the CSEP per bit plane. We can conclude that bit plane 3 is an ideal choice with high PSNR, low $\Delta PSNR$, and good CWEP. As a result, we chose this bit plane for our data set tests.

To demonstrate the effect of different ROI extracted features, we fixed BPP at 1 and chose the third bit plane. In Figure 10, we see that $PSNR$ is nearly fixed for all features. $\Delta PSNR$ is also very good for all ROI features (below 0.6 dB).

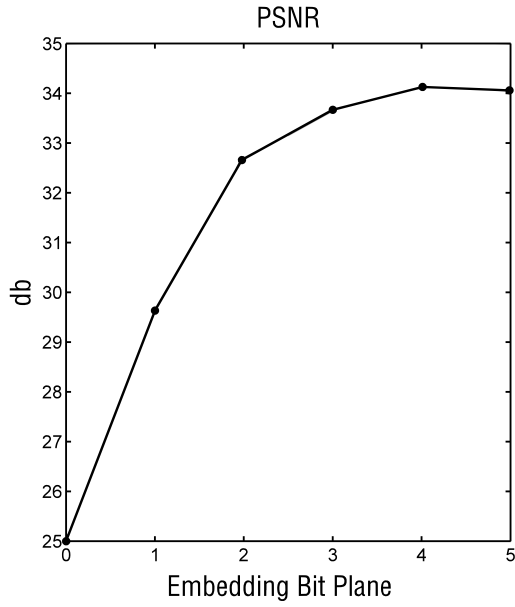
All of the features show superior CWEP results (Figure 11). However, if we pay more attention to the definition of extracted features and their role in the extracting signature, we find that the robustness of a feature is completely related to its CSEP. Figure 11 shows that feature 6 has this characteristic exactly. This feature also has higher CWEP compared with feature 5. For this reason, we chose feature 6 in our method, too.

Moreover, the change of cut-off frequency shows little effect of this factor on $PSNR$ (Figure 12). Since the ROI size is small compared with that of the ROB, and the extracted signatures amount is less than the minimum available embedding place, the decrease in cut-off frequency from 75 % to 25 % had little effect on $PSNR$.

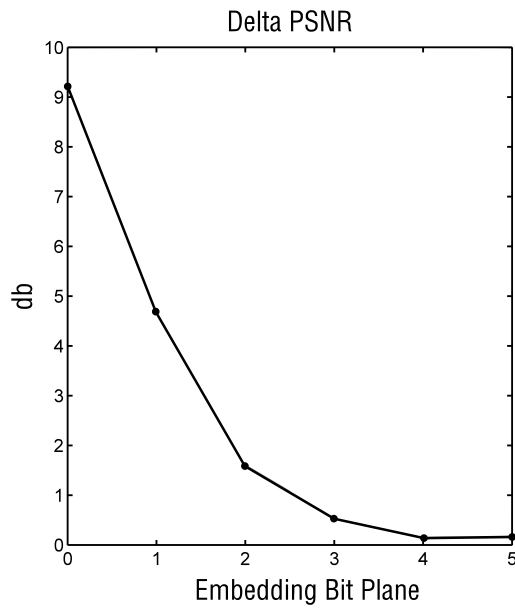
In BPP equal to 1, CWEP is similar in all cut-off frequencies (Figure 13). We chose cut off frequency as 75 %. In this way, watermarks are embedded in places where the eye has the least sensitivity; thus, less distortion is viewed.

6 CONCLUSION

The test results of the proposed algorithm on a large MRI dataset show its general advantages. The simulation was done on a data set including 110 MRI images. When compression was needed, a JPEG2000 algorithm is applied. The size of images and their ROIs were 256×256 and 113×113 , respectively, while the ROI was



a)



b)

Fig. 8. a) $PSNR$ and b) $\Delta PSNR$ as a function of embedded bit plane for BPP equal to one

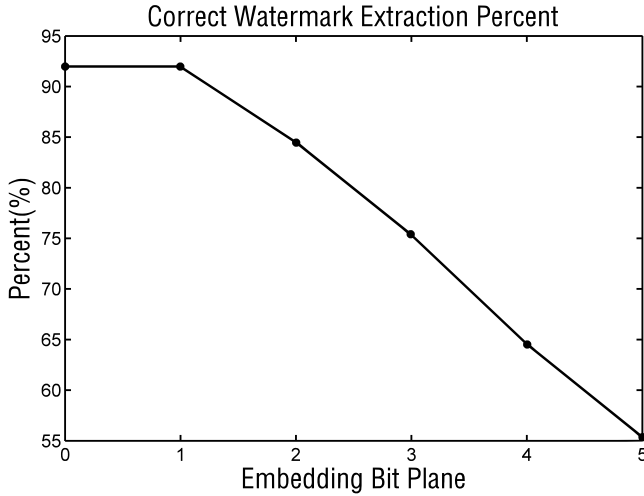


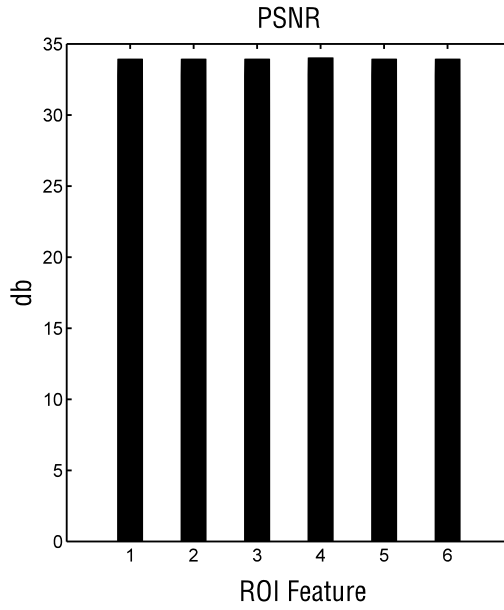
Fig. 9. CWEP as a function of BPP for bit plane #3

again selected in the middle of each image. The following results were captured after averaging the values over 110 images. The result of applying our proposed method in different BPPs ([0.250.51.01.52.04.0]) is shown in Figure 14. The algorithm parameters were selected during the specific tests.

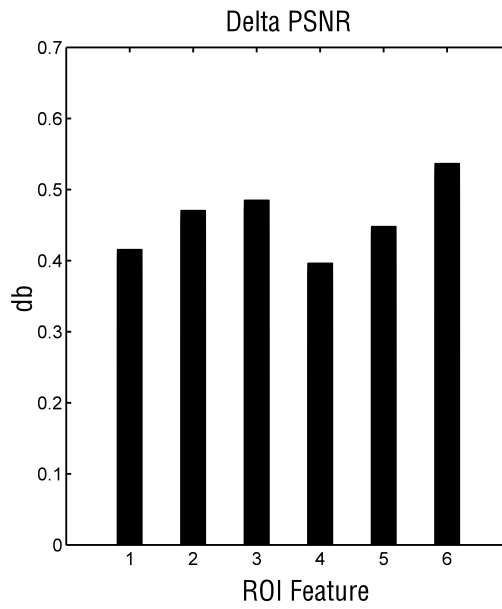
As shown in Figure 14 a), the proposed method on average has a CWEP of more than 85% for BPPs of more than 1.5. This means that our proposed method leads to the content integrity verification of ROI for these BPPs and thus satisfies our watermarking goal. Figure 14 b) shows that our method also has a very high percentage of CSEP (over 95%). The $PSNR$ and $\Delta PSNR$ values are also acceptable for all BPPs (Figures 14 c), d)). For example, in $BPP = 1$, the distortion effect of watermarking is less than 1 dB. Thus, we can conclude that our proposed method is strong with high fidelity and robustness against compression, i.e. this method not only leads to high CWEP but also to very good $PSNR$.

Figure 15 shows the result of embedding the watermarks based on our method in different bit planes (0 to 5). In our experiments, we fixed BPP at 1 and selected the sixth features and cut-off frequency at 75%. In bit plane 2, the CWEP is over 85%, which satisfies our predefined threshold for integrity verification. In bit plane 3, this amount is near to the threshold (82.5%). This observation does not confirm our previous assumption about choosing bit plane 3. Since $PSNR$ is also high (less than 2.5 dB) at bit plane 2, we chose this bit plane for embedding.

We conclude that our proposed method not only has good CWEP in different BPPs but also very low distortion. Using an HVS-based model, our method embeds watermarks in places to which the eye has the least sensitivity. We propose the following suggestions:

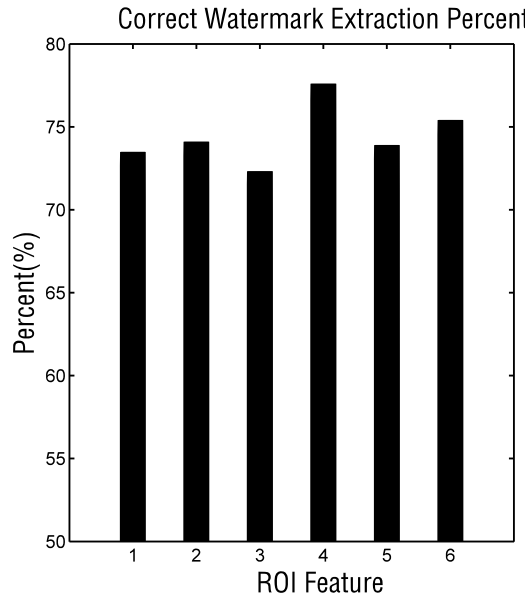


a)

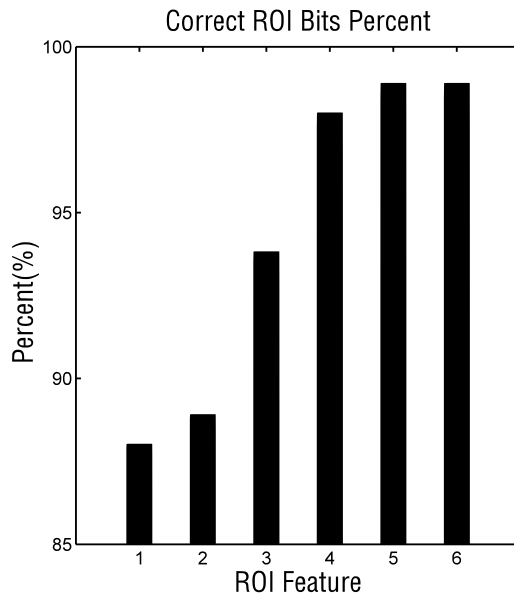


b)

Fig. 10. a) $PSNR$ and b) $\Delta PSNR$ in different features for BPP equal to one and bit plane #3



a)



b)

Fig. 11. a) CWEP and b) CSEP in different features for BPP equal to one and bit plane #3

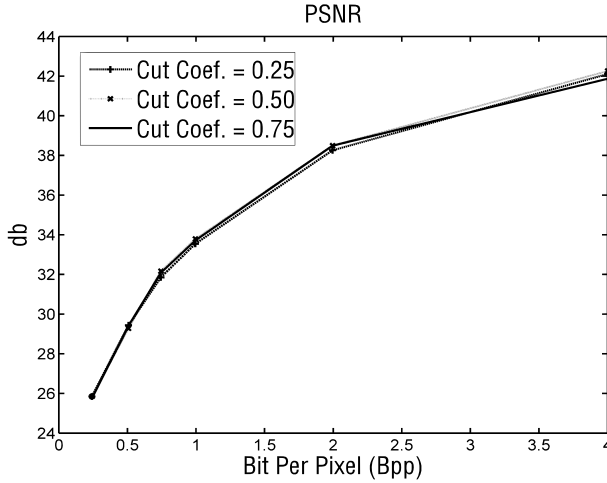


Fig. 12. *PSNR* as a function of BPP for different cutoffs, BPP equal to one, feature #6 and bitplane #3.

- use of time-frequency transforms other than multi level DWT
- working on how JPEG2000 quantization works, so that maximum CWEP could be obtained meanwhile *PSNR* is high
- extracting other robust to compression ROI features, so that maximum CSEP would be achieved.

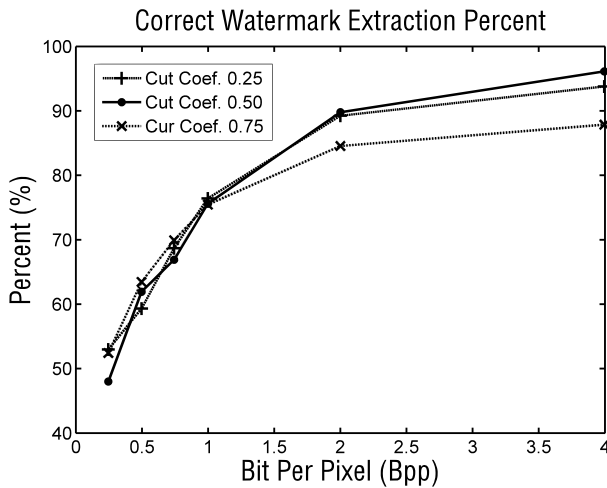


Fig. 13. CWEP as a function of BPP for different cutoffs, BPP equal to one, feature #6 and bitplane #3.

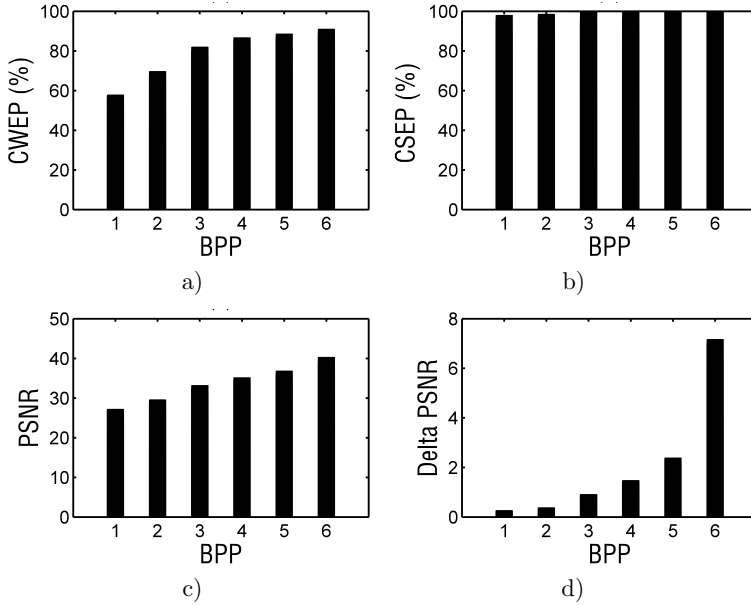


Fig. 14. CWEP, CSEP, $PSNR$, and $\Delta PSNR$ for different values of BPP (0.25, 0.5, 1.0, 1.5, 2.0, and 4.0), bit plane #3, feature #6, and cutoff frequency equal to 0.75 %

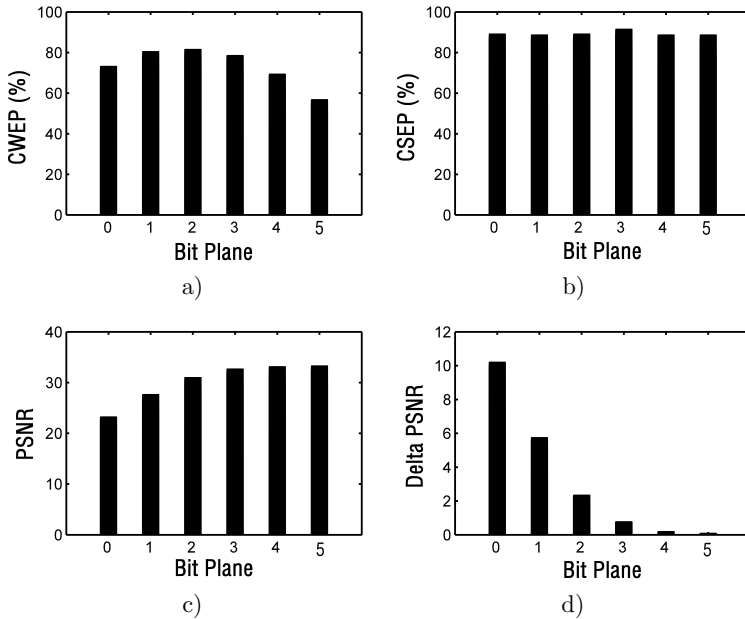


Fig. 15. a) CWEP, b) CSEP, c) $PSNR$, and d) $\Delta PSNR$ for different bit planes of BPP (0, 1, 2, 3, 4, and 5), BPP equal to one, feature #6, and cutoff frequency equal to 0.75 %

REFERENCES

- [1] WOOTEN, R.—CRAIG, J.—PATTERSON, V.: *Introduction to Telemedicine*. Rittenhouse, London 2006.
- [2] KAIDU, M.—TOYABE, S. et al.: Development and Evaluation of a Teleradiology and Video Conferencing System. *Journal of Telemedicine and Telecare*, Vol. 10, 2004, No. 4, pp. 214–218.
- [3] PALOMBO, A.—FERGUSON, J. et al.: An Evaluation of a Telemedicine Fracture Review Clinic. *Journal of Telemedicine and Telecare*, Vol. 9, 2003, Supplement 1, pp. 31–33.
- [4] KOFF, D. A.—SHULMAN, H.: An Overview of Digital Compression of Medical Images: Can We Use Lossy Image Compression in Radiology? *Can. Assoc. Radiol. J.*, Vol. 57, 2006, No. 4, pp. 211–217.
- [5] COATRIEUX, C. G.—LECORNU, L.—ROUX, CH.—SANKUR, B.: A Review of Image Watermarking Applications in Healthcare. *Embc 2006: IEEE Int. Conference on Engineering in Medicine and Biology*, New York 2006.
- [6] VOYATZIS, G.—NIKOLAIDIS, N.—PITAS, I.: Digital Watermarking: An Overview. *IX European Signal Processing Conference (EUSIPCO '98)*, Rhodes, Greece, Vol. 1, 1998, pp. 9–12.
- [7] COX, I. J.—MILLER, M. J.—BLOOM, J. A.: Watermarking Applications and Their Properties. *Proceedings of the IEEE International Conference on Information Technology: Coding and Computing*, pp. 6–10, 2000.
- [8] FRIDRICH, J.: Image Watermarking for Tamper Detection. *Proceedings of the IEEE International Conference on Image Processing*, Vol. II, Chicago, IL, USA, October 1998, pp. 404–408.
- [9] KAI, X.—JIE, Y.—MIN, Z.—LIANG, L.: HVS-Based Medical Image Compression. *European Journal of Radiology*, Vol. 55, 2005, No. 1, pp. 139–145.
- [10] MARR, D.: *Vision*. Freeman, New York 1982.
- [11] XIE, G.—SHEN, H.: Toward Improved Wavelet-Based Watermarking Using the Pixel-Wise Masking Model. *Proc. of IEEE Int. Conf. on Image Processing (ICIP)*, Vol. 1, 2005, pp. 689–692.
- [12] FRIDRICH, J.—GOLJAN, M.—BALDOZA, A. C.: New Fragile Authentication Watermark for Images. *24 IEEE Int. Conf. on Image Processing (ICIP)*, Sep. 2000, Vol. 1, pp. 446–449.
- [13] ANAND, D.—NIRANJAN, U. C.: Watermarking Medical Images With Patient Information. *26 Annual Int. IEEE Conf. of Engineering in Medicine and Biology Society*, Vol. 20, 1998, No. 2, pp. 703–706.
- [14] KONG, X.—FENG, R.: Watermarking Medical Signals for Telemedicine. *IEEE Transactions on Information Technology in Biomedicine*, Vol. 5, 2001, No. 3, pp. 195–201.
- [15] MAEDER, A. J.—PLANITZ, B. M.: Medical Image Watermarking for Multiple Modalities. *34th Applied Imagery and Pattern Recognition Workshop: Multi-modal Imaging*; Washington DC., 2005, pp. 158–163.

- [16] KUNDUR, D.—HATZINAKOS, D.: A Robust Digital Image Watermarking Method Using Wavelet-Based Fusion. *IEEE Int. Conf. on Image Processing (ICIP)*, Sept. 1997, Vol. 1, pp. 544–547.
- [17] SANCHEZ, V.—MANDAL, M.—BASU, A.: Robust Wireless Transmission of Regions of Interest in JPEG2000. *Proc. of IEEE Int. Conf. on Image Processing (ICIP)*, Vol. 4, 2004, pp. 2491–2494.
- [18] LIN, C. Y.—CHANG, S. F.: Semi-Fragile Watermarking for Authentication JPEG Visual Content. *SPIE 10 International Conference on Security and Watermarking of Multimedia Contents II*, Vol. 3971, USA 2000.
- [19] COX, I. J.—MILLER, M. L.—BLOOM, J. A.: *Digital Watermarking*. Morgan Kaufmann Inc., San Francisco 2002.
- [20] OSBORNE, D.—ABBOTT, D.—SORELL, M.—ROGERS, D.: Multiple Embedding Using Semi-Fragile Watermarks for Wireless Medical Images. *Proceeding of the IEEE Conference “Electronics and Telecommunications” (ETC-2004)*, Timisoara, Romania, October 22–23, Section 13 (34), pp. 120–125.
- [21] SERDEAN, C. V.—AMBROZE, M. A.—TOMLINSON, M.—WADE, G.: Combatting Geometrical Attacks in a 18 DWT Based Blind Video Watermarking System. *Proceedings of the 4th EURASIP-IEEE International Symposium on Video, Image Processing and Multimedia Communications*, 2002, pp. 263–266.
- [22] SUHAIL, M. A.—OBAIDAT, M. S.—IPSON, S. S.—SADOUN, B.: A Comparative Study of Digital Watermarking in JPEG and JPEG 2000 Environments. *Information Sciences – Informatics and Computer Science: An International Journal*, Vol. 151, 2003, pp. 93–105.
- [23] WAKATANI, A.: Digital Watermarking for ROI Medical Images by Using Compressed Signature Image. In *Proc. of 35th Hawaii International Conference on System Sciences*, 2002, pp. 2043–2048.
- [24] LIE, W. N.—HSU, T. L.—LIN, G. SH.: Verification of Image Content Integrity by Using Dual Watermarking on Wavelets Domain. *IEEE Int. Conf. on Image Processing (ICIP)*, Sept. 2003, Vol. 2, pp. 487–490.
- [25] LEE, H. K.—SONG, G. S.—KIM, M. A.—YOO, K. S.—LEE, W. H.: A Digital Watermarking Scheme in JPEG2000 Using the Properties of Wavelet Coefficient Sign. *Conference Proceedings of Computational Science and its Applications (ICCSA)*, 2004, Vol. 1, pp. 159–166.
- [26] LEWIS, A. S.—KNOWLES, G.: Image Compression Using the 2D Wavelet Transform. *IEEE Transactions on Image Processing*, Vol. 1, 1992, No. 2, pp. 244–250.



Emad FATEMIZADEH received the B.Sc. degree in electrical engineering (electronics as major) from the Sharif University of Technology, Tehran, Iran in 1991 and the M.Sc. degree in biomedical engineering from Amir-Kabir University of Technology in 1994. He received his Ph. D. degree in electrical engineering from Tehran University in 2003. In September 2004, he joined the Faculty of the Biomedical Engineering Group, Department of Electrical Engineering at the Sharif University of Technology at Tehran, Iran. His research interests include medical image analysis and processing and pattern recognition. His research

field spans a range of topics in image processing including image registration, segmentation, watermarking, steganography, texture analysis, and content-based image retrieval. He is a member of the IEEE and founder and member of Iranian Society of Machine Vision and Image Processing (ISMVIP).



Mona MANESHI received her B.Sc. degree in electrical engineering (communication as major) from Shiraz University, Iran in 2004. She finished her M.Sc. in biomedical engineering at Sharif University of Technology in 2007. She is currently Ph. D. candidate in biomedical engineering at McGill University. Her current research focuses on the application of functional and anatomical connectivity in epilepsy.